

Trajectory Inference for Single Cell Omics

Alexandre Hutton, Jesse G. Meyer

Department of Computational Biomedicine, Board of Governors Innovation Center, Advanced Clinical Biosystems Research Institute, and the Smidt Heart Institute, Cedars Sinai Medical Center, Los Angeles CA 90048, USA

Correspondence to alexandre.hutton@cshs.org or jesse.meyer@cshs.org

Abstract

Trajectory inference is used to order single-cell omics data along a path that reflects a continuous transition between cells. This approach is useful for studying processes like cell differentiation, where a stem cell matures into a specialized cell type, or investigating state changes in pathological conditions. In the current article, we provide a general introduction to trajectory inference, explaining the concepts and assumptions underlying the different methods. We then briefly discuss the strengths and weaknesses of different trajectory inference methods. We also describe best practices for using trajectory inference, such as how to validate the results and how to interpret them in the context of biological knowledge. Finally, the article will discuss some of the applications of trajectory inference in single-cell omics research. These applications include studying cell differentiation, development, and disease. We provide examples of how trajectory inference has been used to gain new insights into these processes.

Introduction

Omic time courses are of particular interest for understanding the molecular changes that lead to the cellular basis for the progression of disease or identifying predictive markers for pathologies. However, most approaches to single-cell research, such as proteomics or transcriptomics, are inherently destructive to the cells of interest, making it impossible to track a cell's changing omic profiles across time. To address this, computational methods have been developed to stitch together separate samples and order them along a trajectory derived from the cell similarities. The ordering, referred to as "pseudotime," simulates the progression of a cell away from a reference cell state, which can have multiple branching paths.

A simple application is cell differentiation: starting from a stem cell differentiating into multiple cell types, the omic profile will change as progenitor cells transition to cells with specialized functions. One pathway for hematopoiesis, for example, differentiates from hemocytoblasts, to myeloid progenitor, and into megakaryocytes or erythrocytes (among others). The omic profiles of hematopoietic stem cells differ from their descendants [1]; one could sample cells along the trajectory and order their omic profiles according to their position in the lineage relative to the hemocytoblasts.

However, it is not usually possible to link omic profiles to specific points in a lineage. Given the heterogeneity and noise of single-cell omic profiles [2], matching an observed profile to a known profile can't be done with certainty. In experiments exploring novel pathologies or rare cellular subtypes, it can't be done at all. Instead, trajectory inference aims to connect cells by the similarity of their omic states (**Figure 1**). The rationale is that for a given cell type, there will be a distribution of biologically-functional omic profiles, and that as cells transition from one state to another, that distribution of those profiles will shift. One of the core assumptions across trajectory inference methods is that enough cells are sampled so as to capture the whole transition; otherwise, gaps could lead to ambiguous trajectories that could link trajectories between omicly-similar cells that are not part of the same lineage.

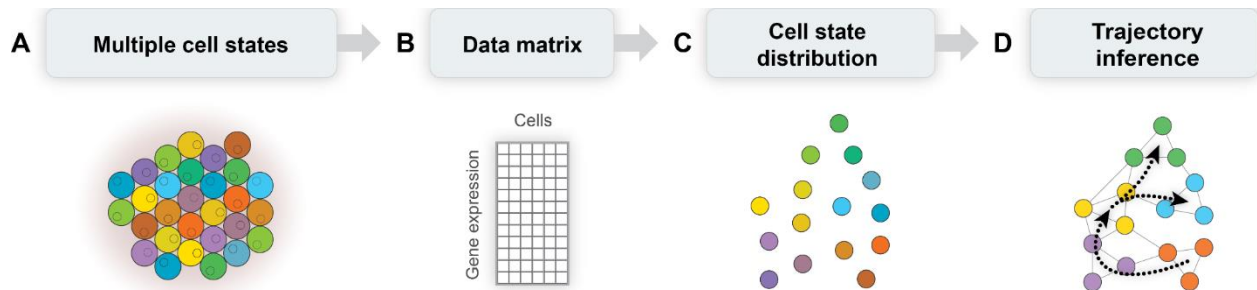


Figure 1. Trajectory inference concept. **(A)** A single cell suspension is generated from a complex biological system with multiple cell states. **(B)** Single cell omic data is obtained from the cell suspension, producing a data matrix of quantities related to genes across all measured cells. **(C)** The omic data is used to derive a cell state distribution that is usually portrayed in dimension reduced space where cells may be clustered by similarity. **(D)** Trajectory inference methods infer the relationships between cells that may indicate development or progression to disease states.

There exists reviews on the transcriptomic methods [3], [4] that cover various methods for inferring trajectories; while this review will offer an overview of these methods, the purpose of this paper is to review where these methods have been applied, how they can be best applied to future studies, and discuss some pitfalls that could impact the interpretation of their results.

Methods Overview

Trajectory Inference

There are a variety of tools for performing trajectory inference; Monocle, Slingshot, and PAGA are the most-cited packages (**Figure 2**). We note that Monocle and Slingshot, the two most-cited packages, are made for R, while PAGA and Palantir are implemented in Python. Knowing that R (and more specifically Bioconductor [5]) is widely used in bioinformatics, it would make sense for the packages in R to be adopted more quickly. We also note that Monocle 1-2 is likely to be overrepresented since the Monocle packages require citing their previous versions. In this section, we offer a summary of how the most-cited methods work in the hope that a better understanding will aid users in knowing what information can be extracted from results and when to be wary.

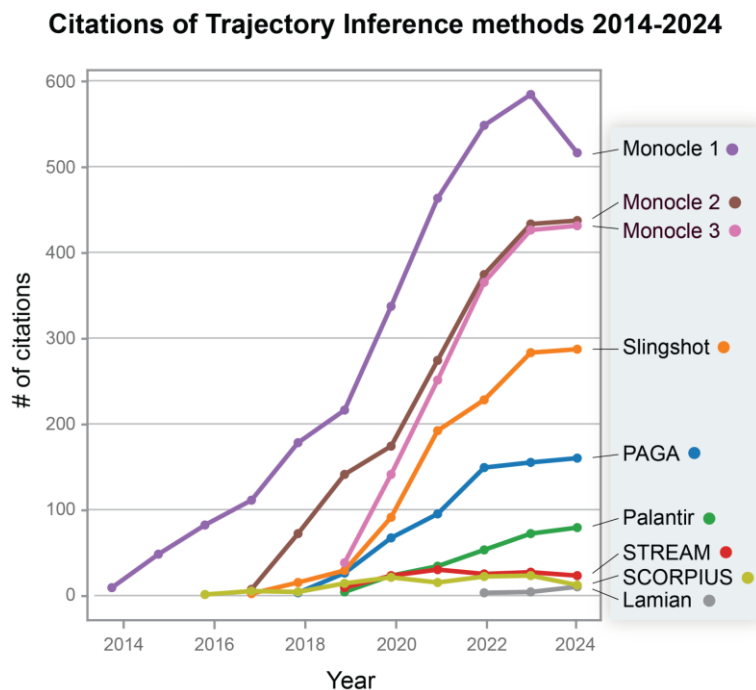


Figure 2. Citations for the various trajectory inference software packages over time.

Slingshot (2018)

Slingshot [6], introduced by Street *et al.*, uses a method for trajectory inference that is similar to Monocle 1 [7] and 2 [8], with some key differences that optimize robustness against sources of noise, modularity of use with different pre-processing steps, and better identification of multiple lineage branchings.

Monocle uses a minimum spanning tree (MST), where its implementation fits all available data

points. When the computed pseudotime for a given dataset was compared to that of a subsampled set, Street *et al.* found that the pseudotime ordering changed dramatically compared to other methods and concluded that the approach was not sufficiently reliable. By contrast, methods using principal curves[9] to compute pseudotime were most stable against

subsampling, but are not able to account for branching lineages. To address this, Slingshot computes a MST from clusters in the data instead of using the data directly, and then computes a curve for each trajectory; the MST allows for flexibility of branching lineages while the principal curve offers robustness to noise and generalizability to similar datasets. Once the curves are obtained, pseudotime for each sample is computed by projecting it to the closest curve and evaluating its distance along the curve from the user-specified starting cluster. A marked difference between Slingshot and other approaches is its ability to fit into different workflows; Slingshot assumes that the data is clustered, but it does not require a specific clustering to function. Street *et al.* evaluated different clustering methods with different total clusters and found that although performance decreased quickly at low cluster counts and dropped off gradually as the counts increased, it was comparable across both clustering method and parameters.

Partition-based graph abstraction (2019)

Partition-Based Graph Abstraction (PAGA) [10] is an algorithm for discovering relationships present within single-cell RNA-seq (scRNA-seq) data. There are generally two approaches to representing single-cell data: clustering and continuous transitions. While clustering approaches present us with an intuitive interpretation of distinct cell groupings (e.g., cell types) that can be determined by a cell's transcriptome, it has some limitations. Single-cell experiments regularly demonstrate that the different omic profiles are heterogeneous, even among specific and known cell types; if a cell differentiates into a different cell type, its transcriptome will change continuously to be more like its new type, but it is unclear where along that transition it should be labeled as its new type. It is also unclear how cell similarity can be evaluated reliably. For example, take a cell that differentiates multiple times with a terminal state similar to its starting state (**Figure 3**), evaluating similarity using inter-cluster distances would place the final cell type "closer" to its starting type than its intermediate states. By contrast, continuous approaches to identifying connections paint a richer picture of the variability of omic profiles, but make some assumptions about the data distribution that don't generally hold as follows. The core assumption is that the underlying processes are accurately captured by the data, which is less likely to be true for rapid transitions. In cases where the process is not sufficiently well-sampled, the trajectory between cell states could be misrepresented.

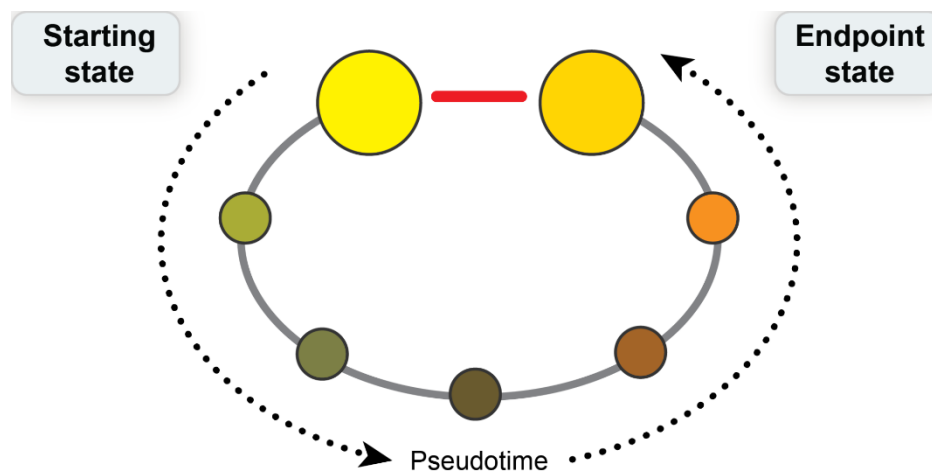


Figure 3. Schematic of inter-cluster distances in 2D space. By judging the space using only the distances in gene space between clusters, we might conclude that the two top-most clusters are linked. Instead, treating the process as continuous and inferring a trajectory would reveal that there are intermediate stages through which cells transition before reaching the terminal state.

Continuous trajectory inference methods are also ill-equipped to deal with unconnected sections of the data. If multiple unrelated cell types are present in the data, these methods, the assumption is that these should nonetheless be connected on the same trajectory. This is particularly problematic when dealing with in vivo samples where multiple cell types are likely to be present despite having separate lineage and functionality.

PAGA combines the clustering and continuous approach. Although previous methods also represent the data as graphs, single-cell data's noisy nature and sparse sampling make it difficult to determine which cells should be grouped together. By using a multi-resolution approach to creating the graph and statistical model for node (cluster) connectivity, PAGA is able to accommodate data distributions that are more in line with single-cell data, including disconnected clusters, sparse sampling, and continuous changes between cell states. See the supplementary GitHub repository with a tutorial notebook demonstrating and explaining the usage of PAGA (https://github.com/xomicsdatascience/trajectory_review/).

Monocle (2014, 2017, 2019)

Monocle is a toolkit created for analyzing single-cell RNA-seq data (scRNA-seq), including clustering, differential expression, and trajectory inference. It is currently on its third iteration. Monocle 1 [7] introduced trajectory inference. Monocle 2 [8] improved scalability, particularly by supporting sparse matrices, and updated the trajectory inference to use reversed graph embedding to reconstruct trajectories. The latest iteration, Monocle 3 [11], the toolkit expanded its applicability to large datasets (on the order of millions of samples) while removing some assumptions made by the underlying implementation and allowing trajectories to better fit the variety of cell behaviours and observed datasets (multiple origins, cell state cycles, converging cell states from different origins). Monocle projects the high-dimensional scRNA-seq data to a low dimensional state using UMAP[12], which allows for local distances to be computed more efficiently and preserves the global structure of the data. Clustering is then performed using the Louvain algorithm to identify groups with similar expression patterns. Using these groups, a graph is constructed using a variant of the SimplePPT algorithm [13], [14] to allow it to use principal curves on large datasets and to produce a graph containing loops. From there, pseudotime values are computed by projecting each sample onto the trajectory and computing the distance from a root node. In the case of multiple root nodes, pseudotimes are taken as the minimum distance across all root nodes. See the supplementary GitHub repository for a notebook tutorial of Monocle usage with notes (https://github.com/xomicsdatascience/trajectory_review/).

Palantir (2019)

Palantir [15] is an approach that treats cell trajectories as primarily continuous, whereas previous work had treated them as transitions between discrete states. Since single-cell omic studies have shown that cell transitions appear to steadily shift from the omic profile of one state towards the profile of the other, and that since discrete borders are not immediately apparent, it is reasonable to treat cell types as a continuum.

To compute trajectories, Palantir first places the data into a low-dimensional space using a kNN graph using diffusion maps (**Figure 4**) [16]. Diffusion maps can be made to better model the similarity between cells by including a similarity function that transforms the distance in some way; based on previous work, Palantir uses an adaptive Gaussian kernel to transform the Euclidean distance. Typically, a Gaussian kernel has a fixed width (variance) and penalizes the similarity of two cells exponentially as a function of the Euclidean distance between them. Knowing that the density of cells along a trajectory is usually variable (more cells in stable states, fewer in transition areas), the group instead opted to use an adaptive kernel whose width varies with the density of samples, allowing for variable densities and making trajectories more stable. To compute pseudotime along these trajectories, the direct approach of accumulating shortest-path distances from the origin to other cells has been found to accumulate noise as the total distance increases. To limit this impact, distances are instead computed from the nearest waypoint, which are distributed uniformly along the estimated trajectories. The core to Palantir's approach is to then use these waypoints as states in a **Markov chain**, establish directionality using the computed pseudotime, and identify terminal states. **Markov chains** model the

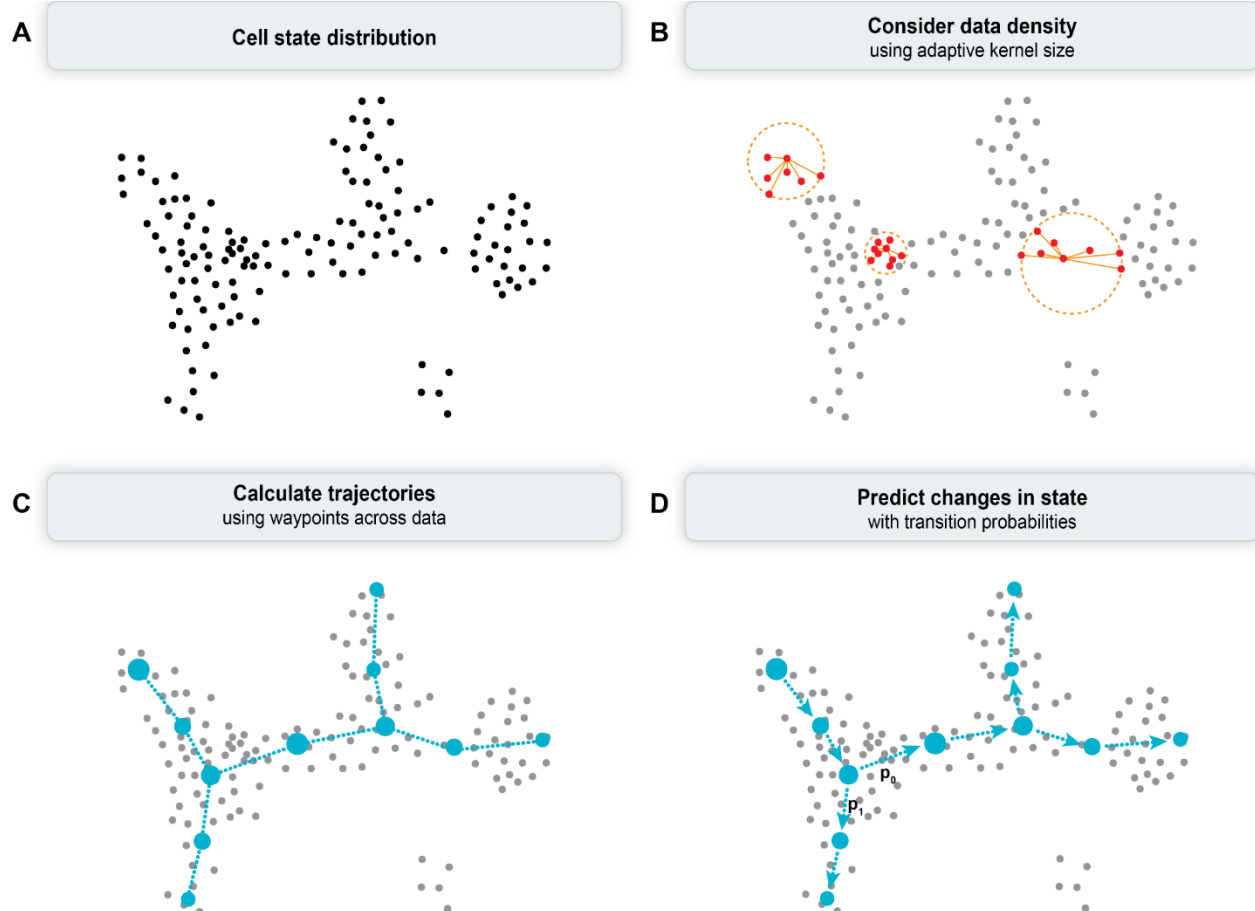


Figure 4. Steps used by Palantir for determining trajectories. (A) Distribution of data sample. (B) Using an adaptive Gaussian kernel, the distance between cells is obtained and used to obtain a diffusion map. (C) Using the obtained distances, waypoints are distributed evenly throughout the space. (D) Transition probabilities are computed, modeling the chance that a cell in one state transitions to downstream states. These probabilities are later used to compute the entropy of a state.

transition from one state to another using a transition probability matrix, and that transition matrix depends only on the current state; this states that all information from previous states that might affect the transition matrix is also present in the current state. The Markov chain is directly comparable to the underlying cells. Finally, the group defines the **differentiation potential** for each state within the Markov chain as the entropy of each state computed using the probabilities of a state reaching different terminal states. In the context of modeling cell differentiation, entropy is *high* when there are multiple terminal states that can be reached from the current state, and entropy is *low* when there are fewer possibilities. Differentiation potential reflects how well one can predict where the cell will end up; high potential is low predictability and vice versa.

Interactive tutorial notebooks

Tutorials for Monocle using R and PAGA using Python are available on GitHub (https://github.com/xomicsdatascience/trajectory_review/). Using the data for the Paul *et al.* 2015 [17] paper commonly used in Scanpy [18], we demonstrate how to process data and obtain trajectories (**Figure 5**). Note that although there is a general agreement between trajectories, the pseudotime estimates¹ do differ.

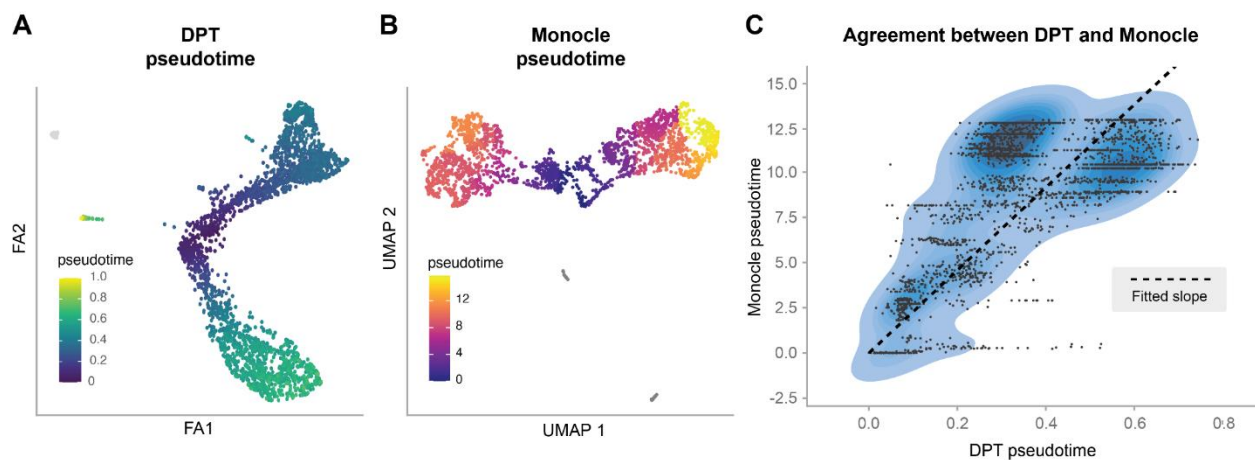


Figure 5. Pseudotime estimates computed for the same dataset using different methods. **(A)** Diffusion pseudotime computed with Scanpy. Data is projected on Force Atlas axes, a method for determining a graph layout. **(B)** Pseudotime computed by Monocle 3 projected onto UMAP axes. **(C)** Scatterplot comparing pseudotime from the two methods.

Computing Pseudotime

Although related, trajectory inference and pseudotime are different methods. Whereas trajectory inference is used to estimate how cell states change across gene space, pseudotime is a

¹ For PAGA, pseudotime estimates were obtained using diffusion pseudotime [19], [10].

distance metric that measures distances relative to some origin. Pseudotime should be considered as a measure of omic change along some trajectory rather than a measure of time, and external information is required to connect pseudotime to actual time or some kind of progression. At its simplest, one could compute the Euclidean distance between an origin and all other samples and this would constitute a valid value for pseudotime by definition, though not likely a useful value. Inferred trajectories are useful for making more reliable estimates of pseudotime; distances for a given sample represent the distance between the origin and a point on the trajectory to which a sample is mapped. To compute pseudotime, Monocle² [11] first computes a trajectory for a given dataset and projects each sample onto its nearest point on the trajectory. From there, a sample's pseudotime is the geodesic distance along that trajectory; that is, the sum of the distances between successive points that are on that trajectory starting from a specified root. By contrast, methods such as diffusion pseudotime (DPT) [19] compute pseudotime by selecting a root, applying a distance kernel to estimate distances and obtaining transition probabilities (the probability of a sample transitioning to a nearby state), then using the geodesic distance from a root cell to each sample. From the computed pseudotimes, DPT would then use patterns³ in those values to identify branching points and produce a trajectory.

General Assumptions

Although each method makes separate assumptions in their approaches, there are general assumptions that are common across the different methods.

Sampling. The biological process being observed should be sufficiently sampled so that all parts are represented in the collected dataset, including transition states (**Figure 6**). Given the variety of processes, it is not possible to prescribe specific numbers. Tools such as SCOPIT [20] can offer estimates for the required number of samples when seeking rare cell states, but since one does not usually have values for the necessary inputs, the values they produced may not reflect the best experimental protocol. A discussion of statistical power considerations in single-cell experiments has been previously published by Jeon et al. [21]. The limitation is present even when observing known processes; cell transition states (e.g., partway through differentiation) will probably be less common than their terminal states. Knowing whether a sufficient number of samples has been collected is likely to be iterative in practice and part of developing an experimental protocol; the important criterion is that there are no large gaps present in the trajectory (and by extension, in pseudotime). To our knowledge, no analysis of what presents a reasonable and acceptable gap has been done, and inference methods will usually use some heuristic (Palantir uses the distance of the n^{th} nearest neighbor, PAGA uses interconnectedness) that has been found to work across different datasets. There is an inherent weakness in this approach: iteratively acquiring data in pursuit of a desirable outcome is

² The implementation changes between Monocle 2 and 3 for computational reasons, but the high-level concept is comparable.

³ Using different origins and repeating the procedure, branches can be detected when the pseudotime values between two different origins change from moving against one another to moving in the same direction.

tantamount to p-hacking. To avoid this, sample count requirements should be estimated in the first phase of an experiment before the collection of the full dataset in a later phase.

Continuity. Although related to sampling, the assumption of continuity does not entirely overlap with sampling. All trajectory inference methods assume that a biological process is continuous in gene-space; their degree of gene expression changes continuously across the process being observed. If this assumption holds, then a sufficiently-sampled process should have cells representing the entire spectrum of cell states.

Consequently, we would conclude that cell states that don't have a line of cells between them are not directly related. This assumption is important to consider when examining gene expression across pseudotime; downstream trajectories are user-identified from computed nodes or clusters and are identified due to some biological question being explored (e.g., one could have a hypothesis that cell

A differentiates into B then C, and select nodes or clusters that relate to those cells). If the pseudotime along the selected clusters presents a gap, this indicates that either (1) the process is insufficiently sampled, (2) the trajectory is missing an intermediate state, or (3) the cells are not directly related. Examples for (1) are straightforward: the biological process is present, but more samples are required to observe it. For (2), a user could select hematopoietic stem cells and macrophages from their dataset; the data is sufficiently sampled and they are part of the same lineage, but intermediate stages were not selected. Lastly, (3) the selected clusters are not directly connected to one another due to being from entirely different lineages or on different branches from a common ancestor.

Pseudotime is dimensionless. Pseudotime is an ordering of samples relative to some start. Since no units are associated with it, its value is largely arbitrary. Some methods normalize it to the $[0,1]$ range to make the extreme values consistent across applications, while other implementations keep the index of the sample order. Consequently, different portions of pseudotime are not directly comparable across datasets; for example, if one dataset contains descendants that another does not, the cell state distributions across pseudotime would shift despite there being no other underlying difference (**Figure 7**).

Connecting pseudotime to time or progress

Trajectory inference identifies cells that are close to one another in gene space and proposes a path through the dataset to connect different cell states. However, it is not possible for these

Expected frequency of cell states along trajectory

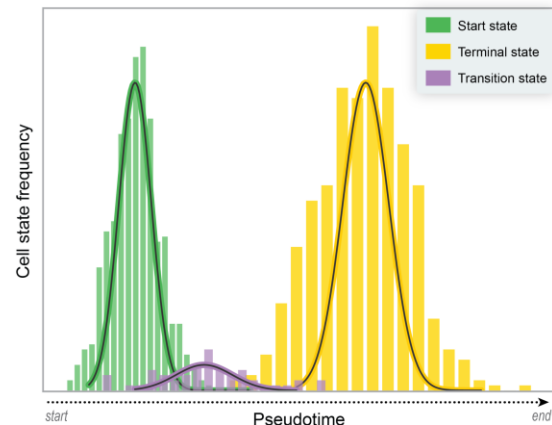


Figure 6. When sampling a biological process, experiments must acquire enough datapoints to detect rare states; for some processes, transitions may be quick and have a low chance of being detected.

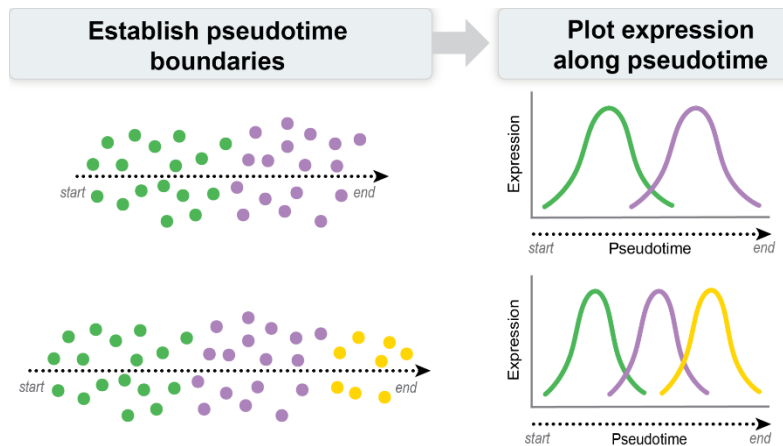


Figure 7. Two almost-identical datasets, with the lower one containing extra cells near the end of the trajectory. Since the trajectories have different endpoints, directly comparing the “middle” or “end” of pseudotime is not meaningful. Methods that don’t normalize pseudotime have a similar problem; adding more samples in one cluster would compress all other clusters in pseudotime.

methods to infer any kind of directionality. Several pieces of external information are required to determine and validate connecting pseudotime to time.

Origin or root cell. A starting point is required to identify the directionality; from a root node, one can set the pseudotime to be 0 and increase it along any connected trajectories. Root nodes are typically selected using gene markers, either for stem cells or some otherwise known starting cell state, such as the healthy state. Most methods support only one root, but some methods can accommodate multiple roots, such as Monocle 3 [22] (by taking the minimum across all roots) or DPT [19] (by taking the average).

Trajectory validation. When investigating a new biological process, it is important to validate computational findings with known markers to ensure that the trajectories can be used to extract new information. The validation can be done by identifying cell types along a lineage and verifying that they have the expected change in biomarkers (e.g., stem cells expressing marker A, then shifting into expressing marker B as they differentiate); one would expect a continuous change in expression in those markers as the cells move through the trajectory. Once parts of the trajectories are validated, examining differences between groups (e.g. disease vs. control) and differences between trajectories can be used to draw conclusions.

Sampling across time. Certain biological processes are better understood by population shifts in cell states. Typical fetal development would contain more stem cells and progenitors than cells in a terminal state, and we would expect fewer progenitors as development progressed. Regardless of other markers, the relative frequency of stem cells to terminal states across developmental stages would itself be a marker for development. Determining these shifts is done by first collecting multiple samples across time, each with their own distribution of cell states along development time. Then one can perform trajectory inference and split the samples by their timestamp. Meng *et al.* [23] correctly used this concept by collecting data from multiple timepoints and found changes in cell subpopulations during neonatal swine development, where progenitors increased while goblet and tuft cells decreased. The change in distribution would otherwise not be possible to demonstrate based on a single time point.

Techniques Enabled With Inferred Trajectories

The computation of cell trajectory relationships opens the ability to perform additional computational analyses. For example, other statistical and information theory techniques like Granger causality and transfer entropy can enable understanding of relationships between molecules across inferred trajectories. Often these approaches attempt to infer gene regulatory networks (GRNs). This area of research is so active that there are robust benchmarking frameworks available [24]. **Figure 8** gives an overview of such applications.

Given a computed pseudotime, we may want to know which genes statistically change along that pseudotime to provide a view of the molecular mechanisms that mediate progression along that pseudotime. Early methods for DE calculation were limited in that they were tethered to specific methods for pseudotime computation, they used generalized additive models and lacked proper estimation of calibrated p-values, or they used general linear models that required invalid assumptions. To solve all these problems, in 2021 PseudotimeDE was introduced, which uses a negative binomial GAM or zero inflated NB-GAM to model uncertainty and improve DE estimation [25]. The paper uses five real-data examples to demonstrate the PseudotimeDE approach. They demonstrate the application of this concept to five datasets. In each of these examples, the authors apply PseudotimeDE along with other DE methods (tradeSeq and Monocle3-DE) and compare their performance based on p-value calibration, power, and functional analysis of the identified genes.

Granger causality estimates whether one time series is causative of another time series. Combining this concept with inferred trajectories of single cell omics data, Granger causality could estimate which molecules influence other molecules over pseudotime. However, due to issues mentioned above related to sparsity in trajectory space and also in missing values of measured molecules, the application of Granger causality to single cell omics trajectories is not trivial. Deshpande *et al.* introduced an approach called SINGE, which is based on kernel-based Granger causality regression that deals with these issues [26]. Importantly, this approach averages an ensemble of regressors to construct a ranked list of regulator-gene interactions. The authors showed superior area under the precision recall curve for detecting known gene regulatory networks from single cell data relative to competing approaches using ESC-to-endoderm differentiation data. The authors further demonstrated good performance of GRN discovery from retinoic acid driven differentiation of mouse embryonic stem cells.

Transfer entropy is a technique from information theory that measures how much information is transferred between two time series datasets. Like Granger causality, transfer entropy also can enable inference of relationships, and is thus another natural analysis technique that can be used to understand the relationships between molecules within an inferred single cell omics trajectory. Kim *et al.* first demonstrated this concept in 2020 with their software TENET [27]. They found superior performance to other GRN inference algorithms when applied to mouse embryonic stem cell differentiation, and also when examining direct reprogramming of mouse fibroblasts into cardiomyocytes. They extensively benchmarked TENET against competitors using Beeline, and found generally very strong performance in predicting targets of transcription

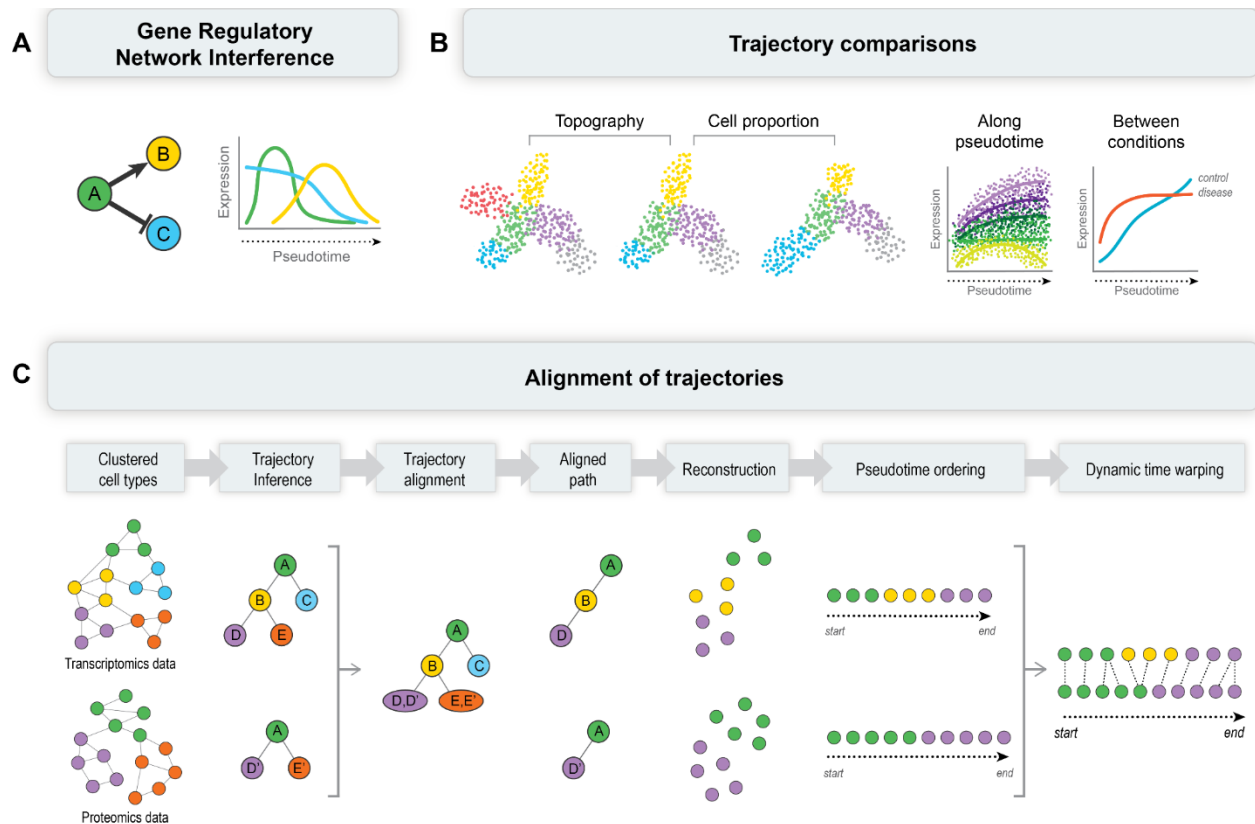


Figure 8. Overview of applications of trajectories. (A) Inferring gene regulation networks from the distribution of gene expressions across pseudotime. (B) Comparison of inferred trajectories between two conditions, including the graph layout of the different conditions or population shifts. (C) Different omic measurements can result in different trajectories; the graphs can be aligned and combined to give a better understanding of the process being analyzed.

factors Nanog, Pou5f1, Esrrb and Tbx3. TENET was even able to discern context specific GRNs, where Nme2 was required for differentiation in 2iL media but not in SL media. Another group recently developed a faster GPU-based implementation of TENET called FastTENET[28].

Given pseudotime trajectories, another task of interest may be to compare trajectories across multiple biological conditions. Hou *et al.* developed the Lamian framework for making statistically rigorous comparisons across groups [29]. The authors claim to overcome two main problems. First their framework can detect a diversity of potential changes in trajectories, which can include (1) topology differences, (2) cell proportion differences, or (3) gene differential expression (DE) changes across mapped cells. Second, their framework can account for separation of biological and technical signals. Their framework includes preprocessing, tree variability estimation, and differential tests along trajectory for gene changes. The authors demonstrated the utility of their package applied to scRNA-seq from bone marrow samples and then applied it to discover differential gene activation in T-cell activation related to COVID-19 infection.

CAPITAL (Comparative Analysis of Pseudotime Trajectory Inference with Tree Alignment) is a valuable new method for comparing single-cell trajectories, even when those trajectories include

branches [30]. Trajectory alignment across single cell omics datasets may be valuable for several reasons, for example comparing the dynamics of gene expression across species, comparing trajectories generated separately for across control and perturbation to discover differential regulators, detecting cell type diversity changes between conditions, or for understanding multi-omic trajectory differences in data measured from parallel cell populations. Existing tools primarily focus on aligning single lineages across datasets with dynamic time warping, which makes them unsuitable for comparing branching trajectories. CAPITAL addresses this limitation by first clustering cells in each dataset and then using a dynamic programming algorithm to perform a tree alignment of the clusters across datasets. Once an alignment of the trajectory trees has been obtained, the single cells within each aligned cluster are aligned using dynamic time warping. This approach enables the comparison of branching trajectories in a global fashion without requiring prior knowledge of the linear paths to be compared. The authors demonstrated this approach by aligning trajectories of blood cell differentiation across species and found that common markers of differentiated blood cells, such as IRF7, CSF1, and ELANE, have different magnitudes of change between human and mouse. CAPITAL offers a promising new way to investigate the dynamics of cellular processes such as differentiation, reprogramming, and cell death, as well as to identify regulators of human disease.

Applications of Trajectory Inference

Trajectory inference is a general analysis method that has a wide range of applications. It is intuitive to link the state progression that it describes to a change across time; one of the most common applications is in examining cell differentiation. The information that can be drawn from a trajectory is compounded when combined with measures beyond the measured gene expression. Several of the applications described here use measurements obtained across multiple timepoints to show population shifts along trajectories; others eschew any temporal association and use the obtained trajectories as a metric for disease severity or as a sort of spectrum to identify cell states in new contexts.

In this section, we present a wide variety of research topics from published literature where trajectory inference and pseudotime were used to extract additional information from a dataset. We offer a brief context for the research being done and describe how trajectories were applied within that context.

Cardiomyocytes (CMs). Cardiomyocytes are the contractile cells in cardiac muscle tissue [31]. *In vitro* derivation of cardiomyocytes from pluripotent stem cells (PSC-CMs) do beat spontaneously, but they do not achieve full functional maturity [32] making it questionable whether PSC-CMs can be used as a realistic model of *in vivo* cell function. It was unclear why the cells fail to mature, and Kannan *et al.* [32] investigate this by first generating an scRNA-seq reference of *in vivo* mouse CM from perinatal time periods. They then created comparable samples using PSC-CM and combined the data. When combined, the groups produced distinct clusters, indicating significant differences between PSC-CMs and all stages of *in vivo* CMs. Correcting for these global differences and using trajectory inference, the group found that PSC-

CMs were most similar to early *in vivo* CMs (embryonic, early perinatal) and that they never matured. These results indicate that the dysregulation that causes the difference is likely to be in that time window. Even when the PSC-CMs were compared to early *in vivo* CMs, there remained global differences in their transcriptomic profiles. By combining their results with existing literature, the group determined that the dysregulation of nine transcription factors related to maturation was critical for the failure of PSC-CMs to mature into functional CMs.

Dilated cardiomyopathy. A 2022 study [33] used Palantir [15] to characterize the transcriptomic profiles of patients with dilated cardiomyopathy by looking at the difference in cell compositions across the different states. The analysis used entropy across genes to identify the diversity of cell composition, showing that cells from patients with dilated cardiomyopathy tended towards two highly-differentiated types of cardiomyocytes vs. seven types in healthy donors, with cell states defined by *ARGRL3* and *NPPA/NPPB* expression. In this study, the authors produced entropy vs. pseudotime plots to demonstrate that the differentiation of cells from healthy donors differed from those originating from patients with dilated cardiomyopathy.

Hypoplastic left heart. One study from Ma *et al.* [34] used samples taken from patients with hypoplastic left heart (HLH), with or without heart failure, to create iPSC-derived cardiomyocytes. The group clustered their data using Seurat [35], [36], [37], [38], [39], and used known gene markers to further collapse the clusters into three groups: mesenchymal stem cells (MSC), cardiomyocytes, and fibroblasts. The trajectory computed using Monocle 2 [8] was used to suggest a differentiation pathway from MSC to cardiomyocytes or fibroblasts. Using these clusters, Ma *et al.* performed functional enrichment analysis (GO[40], [41] and KEGG [42], [43], [44]) to identify differences in cluster gene expression between the cell clusters. They then collected blood samples from three groups (control, HLH without heart failure, HLH with heart failure) and used bulk proteomics to quantify proteins between those groups. This data was similarly analyzed to identify the GO and KEGG terms that were enriched to identify hub genes that overlapped between both approaches. By integrating omic results obtained separately from the inferred trajectory of MSCs and from the differential expression of plasma proteins, Ma *et al.* were able to robustly identify genes involved in HLH.

Kidney organoids. Yoshimura *et al.* [45] examined gene regulatory networks in kidney organoids by examining changes in chromatin structure using single-nucleus ATAC-Seq and acquiring samples across multiple days. Examining tubule lineage cells, the group was able to show the differentiation of posterior intermediate mesoderm cells (PIM) separately into renal tubules (TUB) and podocytes (POD), consistent with previous literature. Further analysis showed TUB differentiating into proximal tubule cells (PT), loop of Henle (LOH), and distal nephron (DN) cells. Their work identified HNF1B as the most-enriched transcription factor, and showed that its targets (FXD2 and PKHD1) were consistent with HNF1B expression along proximal tubule differentiation pseudotime.

Aristolochic acid nephropathy (AAN). AAN is a renal fibrosis that can lead to kidney failure [46]. Chen *et al.* [47] sought to combine scRNA-Seq, RNA-Seq, and mass spectrometry-based proteomics to explore omic profile changes in the kidneys. Dividing genes into cytokines,

cytotoxic, and regulatory roles and plotting their expression against pseudotime, they showed an increase in cytotoxic and regulatory genes as cell states became more affected by AAN.

Acute kidney injury (AKI). AKI describes the reaction of nephrons to harmful conditions such as exposure to toxins or reduced blood flow [48]. Patients experiencing AKI can either recover or develop fibrosis and chronic kidney disease. The mechanisms driving nephrons into either recovery or a chronic condition are not well understood, so Kirita *et al.* [48] used snRNA-Seq to quantify gene expression of 26k healthy mouse cells. Using trajectory inference to display proximal tubule lineage and starting the trajectory at injury, most cells recovered to their healthy state, but cells that failed to repair formed a separate branch in the trajectory, with gene ontology terms “cell motility” and “cell migration” identifying the group. An excellent example of how to complement information obtained from trajectory inference was presented by this group in their Figure 2E.

Intestine. The intestine is an organ with a rich variety of cell types that contribute to overall health [49]. Intestine stem cell differentiation is required to renew the intestinal lining every few days. Cells in this tissue therefore are well suited to study trajectories. Hickey *et al.* [49] looked at the gene expression with snRNA-seq and chromatin accessibility with snATAC-seq of four different sections of the intestine and found that cell differentiation pseudotime differs considerably across the different intestine sections. This showed, for example, that *TMPRSS15* increases along cell differentiation trajectories in the duodenum, which serves as an internal control because this gene activates trypsin in the duodenum. They clustered the variable chromatin accessibility and gene expression and found general markers of stem cells, such as *RGMB* and *SOX9*. They also found several clusters for both data modalities for genes representing each tissue type. They further noted that transcription factor motifs were enriched in each differentiation trajectory. Finally, they correlated the pseudotime of chromatin accessibility with the expression patterns of *ETV6* across tissue, noting tissue specific changes in genomic feature accessibility that correlate with this gene's expression.

Meng *et al.* [23] studied neonatal pig intestines to explore cell differentiation in early mammalian development (specifically pigs). The study is of particular interest because they collected comparable samples across the first three weeks of development. The group examined the transition between stem cells and transit-amplifying cells (TA), which was then further divided into TA cells in the G1 and G2 phases of the cell cycle. Using trajectory inference, they were able to demonstrate the predicted differentiation from stem cell, to TA, to TA-G1, and finally to TA-G2, which was consistent with existing literature. The group then divided the samples according to the age of the pig and found rapid increases in the proportion of these undifferentiated cells relative to the other sampled cell types. Similar analyses were performed for enterocyte (intestinal absorption), goblet cells (mucus-secreting), and tuft cells (chemosensory). Using trajectory inference, enterocytes were found to differentiate from their progenitor state to early/late progenitors, then to immature and mature enterocytes. The trajectory for goblet cells was less clear; although three types of goblet cells were identified, their disconnected clustering makes it difficult to infer trajectories. However, paired with their sampling at different ages that showed one goblet cell type to be absent early on and dominant

at later time points, the authors suggest that that type of goblet cell to be the mature version of the cell. Lastly, tuft cells were separated into three subtypes, with the first being closest to progenitors, where trajectory inference predicted a transition from the first cluster to the second, and either remaining in the second or transition to the third.

Neurovasculature. The network of blood vessels in the brain are an important factor in multiple brain pathologies [50]. Wälchli *et al.* [50] analyzed the transcriptomic profiles from fetal, healthy adult, and diseased adult vascular tissues to produce a reference atlas. The group used trajectory inference to first obtain trajectories and used pseudotime as a distance metric between cell omic profiles, starting from large arteries. They refer to this ordering of endothelial cells as the arteriovenous (AV) axis. The trajectories they obtained generally went from large arteries, arteries, arterioles, capillaries, venules, veins, and large veins, reflecting previous findings. The authors define a signature based on the genes showing gradients across pseudotime in their control group; the selected genes include markers for the different vessels, but some were less-specific in the pathological case.

The use of pseudotime directly as a distance metric is useful for discussing the proximity of cells to others along a particular trajectory, but there are limitations to doing so. In order to compare pseudotime orderings across conditions, trajectories should be computed on the dataset containing all conditions rather than separately. Changes along a trajectory can then be better compared by showing those differences across the conditions of interest. In this paper, the authors presented hand-drawn trajectories showing “major trajectory flow” instead of the ones computed by their inference methods. The 2D projections of their data were computed separately for the three conditions being investigated, resulting in a different number of trajectories for each condition. Notably, the pathological condition has its pseudotime scale determined by a cluster (EndMT) that is not part of the described AV axis, placing doubt on whether the differences between the conditions are due to the underlying biology or a quirk of computing the trajectories.

Alzheimer’s disease (AD). AD is a neurodegenerative condition that is marked by the presence of amyloid beta plaques and tau protein tangles. Binette *et al.* [51] investigated differences in the bulk proteomic profile of patients with AD to those without. Although trajectory inference is designed to link single-cell samples to one another, it is possible to generate trajectories from bulk tissue samples; given that pseudotime is a measure of distance in gene space along some trajectory, it is also useful for demonstrating differences across conditions. The group used SCORPIUS [52], a method that produces linear trajectories and uses principal curves similar to Monocle 3 or Slingshot, and obtained measures of pseudotime to show the Z score of proteins differentially-expressed in AD along pseudotime. This demonstrated the association between their pseudotime and the progression from healthy controls to patients with AD, and they were able to show that the behavior of multiple AD-associated markers across pseudotime were consistent with existing literature (e.g. increasing tau tangles, amyloid beta, and decreases in measures of cognition).

Mukherjee *et al.* [53] investigated establishing a temporal model for stages of AD to quantitatively diagnose patients based on transcriptomic profiles. Using manifold learning, they were able to show the progression along pseudotime from healthy subjects to AD using data sampled from the temporal and dorsolateral cortices. By mapping patient data onto the manifold, the researchers were able to visualize measures of disease progression (e.g., Braak score) along the trajectory and establish its directionality.

The progression of AD is complex and affects many different cell types. Dai *et al.* [54] investigated the transcriptomic changes in astrocytes by collecting single-nucleus data. They found that known genes had changing expression across pseudotime; VIM (reactive astrocyte gene) increased across pseudotime while NRXN1 (homeostatic astrocyte gene) steadily decreased.

Parkinson's disease (PD). PD is neurodegenerative and is marked by a loss of dopaminergic neurons in the substantia nigra [55]. Other cell types are also known to be affected, but the mechanisms and consequences are not as well-understood. Smajić *et al.* [55] characterized cell types in the midbrain and described differences between patients with PD and healthy controls. The group identified multiple microglia subpopulations, and used trajectory inference to estimate the progression from glial cells with high P2RY12 expression to states with either high GPNMB or HSP90AA1 expression (where both are markers for glial cell activation).

Liver. The cellular composition of the liver is particularly complex, even in early development [56]. Lotto *et al.* [56] acquired cells from developing livers between days E7.5 (endoderm progenitor specification) to E10.5 (parenchymal and non-parenchymal cells emerge). They used Palantir [15] to demonstrate the different lineages between hematopoietic and endothelial cells starting from the hemangioblast. Originating and terminal state cells were selected based on known genetic markers, and a combination of pseudotime and differentiation potential were used to describe cell differentiation. Using this approach, they are able to suggest that the liver cell lineage can lead to either a terminus or another differentiation decision.

Pancreas. Tosti *et al.* [57] sought to produce an atlas for the human pancreas, noting general difficulties for studying the organ stemming from its role in digestion that can quickly destroy the cells under study. The group used pseudotime to establish relative distances from the base acinar cells and showed the density of different cell types as a function of the distance, with the inferred trajectory indicating that acinar-i act as a hub for transitioning to other cell types. To examine the different states of pancreatic beta cells, Xin *et al.* [58] examined the effects of producing proinsulin (insulin precursor) on the transcriptome. Since proinsulin is prone to misfolding and leads to stress on the endoplasmic reticulum, cells activate the unfolded protein response to reduce its production. The group was able to identify three activated states for proinsulin production (INS) and the UPR: (INS^{high}, UPR^{low}), (INS^{low}, UPR^{low}), and (INS^{low}, UPR^{high}).

Pancreatic cancer. Pancreatic ductal adenocarcinoma (PDAC) is a disease with generally poor prognosis [59]. Zhou *et al.* employed Monocle analysis to determine cell-type transition states

among acinar, transitional, PanIN, and normal ductal populations. The trajectory analysis revealed two distinct transition states originating from acinar cells. One transition involves acinar cells progressing towards the normal ductal cell route, with ADM_Normal cells as an intermediate stage, while the other transition involves cells progressing from acinar cells towards PanIN cells, with ADM_Tumor cells in between. ADM_Normal is a transition state more similar to normal ductal cells and largely lacking genomic alterations, whereas ADM_Tumor is more related to PanIN and exhibits some alterations, including CDKN2A mutations and aneuploidy. The trajectory analysis supports models of acinar origin in human PDAC development, which is consistent with recent studies in mice suggesting acinar-derived tumors are preceded by PanINs, while ductal-derived tumors are PanIN independent.

Diabetes (Type 2). Beta cells in the pancreas are responsible for glucose homeostasis by producing insulin [60]. Bao *et al.* [60] investigated the transcriptomic profiles of these cells between healthy patients and patients with Type-II diabetes (T2D). The inferred trajectory between conditions had three branches; one “normal” which consisted of predominantly healthy patients, one “obesity-like” branch (or INS^{hi} due to upregulated insulin), and a third “T2D-like” where most samples from T2D patients were found (or INS^{lo} due to downregulated insulin). The authors propose that the INS^{hi} branch was likely to consist of damaged beta cells, which is supported by the upregulation of genes connected to endoplasmic reticulum stress that occurs when insulin is misfolded. Contrasting the INS^{hi} and INS^{lo} branches across their trajectories, the group found expression patterns consistent with previous literature including the upregulation of CASP genes (apoptosis) and ATG genes (autophagy) associated with the removal of proteins (e.g., misfolded insulin).

Muscular Dystrophy. Scripture-Adams *et al.* [61] looked at snRNA-Seq to explore transcriptomic differences in a mouse model for Duchenne muscular dystrophy. Due to their size, skeletal muscle cells can have multiple cell nuclei. The results for their mouse model had specialized nuclei that had specialized functions related to the neuromuscular or myotendinous junctions. Trajectory inference was employed to analyze cell populations in both murine and human muscle tissue, with a focus on how these trajectories are altered in Duchenne Muscular Dystrophy (DMD) and in response to exon-skipping therapies. In the context of myolineage development, trajectory analysis of myolineage nuclei confirmed nuclei type identities and revealed detailed developmental stages. The study found that quiescent mdx satellite cells cluster more closely to activated satellite cells, suggesting a disruption of complete quiescence within mdx muscle relative to wild type (WT). Regarding muscle remodeling, trajectory analysis revealed changes in transcriptome and cellular composition among myolineage cell types, with dystrophin deficiency and partial rescue. WT lineage shows a lack of intermediary phases, while mdx muscle demonstrates increased regeneration, and e23AON treatment reduces these intermediary phases, suggesting a reduction in muscle regeneration. For the myeloid lineage, trajectory analysis of intramuscular myeloid nuclei in dystrophic mice indicates a high degree of relatedness, raising the possibility of trans-differentiation of one subset into another in the context of differing muscle micro-environments. The MDSC-like population was more distantly related to differentiated M1 and M2 effector populations, while the M1/M2 transitional cells were equally related to MDSC, M1, and M2, suggesting that M1/M2 are developmental intermediates.

Regarding fibroblast populations, trajectory inference of fibroblast subpopulations revealed an increase in diverse fibroblasts in mdx relative to WT. It was proposed that Fb MME and Fb NMB are intermediates between Fb POSTN1 and Fb CCL11. For macrophage populations, M1/M2 transitional cells, the primary mdx immune population observed, contracts with treatment and takes on a more MDSC-like gene expression profile and exon-skipping treatment might drive M1/M2 transitional cells to become MDSC and/or M2 cells.

Gallbladder cancer. Chen *et al.* [62] looked into gallbladder cancer and evaluated the cell heterogeneity of the microenvironment. Trajectory inference was used to show the gradual transition in the transcriptome from glandular cells to squamous cancer cells. Another group, Zhang *et al.* [63] examined the relationship between gallbladder cancers and the tumor's microenvironment. By establishing a pseudotime starting with macrophages and combining it with GO enrichment analysis, they were able to show that neutrophil-related genes were enriched partway through the macrophages' differentiation trajectory. Consequently, the activation of these genes supports that tumors communicate with nearby immune cells during metastasis.

A third group, Zhang *et al.* [64] examined the tumor microenvironment in context of the ErbB pathway and found different cell populations between tumors with or without ErbB pathway mutations. Of the two types of epithelial cells that they identified, they showed that along a pseudotime trajectory the population shifts from mostly type-1 in healthy states and mostly type-2 in the cancerous state. Critically, they found a branching point between the two states that contained tumor-promoting genes which demonstrates functionality that could be important in tumor growth. The same group later found population shifts in CD4⁺ T cells, showing population shifts from naïve T cells towards Th17 cells, then branching to two different high-Treg states[65]. These high-Treg and low-Th17 states were associated with samples taken in tumors.

Esophageal cancer. Li *et al.* [66] examined the transcriptomic profiles of esophageal squamous epithelial cells. The authors used transcriptomic data made available through The Cancer Genome Atlas [67], identified numerous cell types, and selected the squamous epithelial samples separately. The group then sub-clustered those samples and found three clusters of interest, corresponding to three types of neoplastic squamous epithelial cells: KRT15+, STMN1+, and SPRR3+. Using trajectory inference, they were able to present a branching trajectory that broadly separated the neoplastic cells into different branches. Note that although the authors compute pseudotime values and suggest that the trajectory is reflective of temporal dynamics, the authors do not justify the choice of the KRT15+ cluster as a temporal origin; one could obtain different dynamics by selecting another cluster as the origin.

Fatty infiltration. Fatty infiltration is the deposition of lipids outside of adipose tissue, particularly in muscle or the liver. Their presence in these tissues can cause damage to the surrounding tissue and negatively impact their normal function. For skeletal muscle, the deposition is mediated through a particular differentiation of fibro-adipogenic progenitors (FAPs) [68]. Fitzgerald *et al.* [68] characterized the differentiation of FAPs using scRNA-seq and identified a subpopulation (MME+) that was significantly more likely to exacerbate fatty

deposition after injury (simulated by glycerol injection). The group demonstrated differences between mice with infiltration vs. those without, where they observed an upregulation of gene markers related to adipocytes (e.g. *Plin1*, *Adipoq*, *Pparg*), which demonstrates their differentiation at 5 days post-injection.

In related work, Oprescu *et al.* [69] investigated the dynamics of the cell populations involved in the regeneration of skeletal muscle. The muscle is a composition of multiple cell types, and their relative proportions shift as a result of injury. Previous research [70] suggested that FAPs were involved in fibrosis. By sampling resting muscle as well as immediately after acute injury, the group was able to identify multiple subpopulations of FAPs, two of which were present in resting muscle tissue (*Cxcl14+*, *Dpp4+*) and appeared to both originate from the activated FAPs that were detected shortly after injury as demonstrated by their inferred trajectories. The other population of interest, muscle stem cells (MuSCs), was similarly examined. The group identified 6 subpopulations and used trajectory inference to find that the MuSCs start in a quiescent state at rest (non-injured) and transition into committed, differentiated, or self-renewing states after injury. Beyond the cell state transitions, the paper also demonstrates a population shift during recovery, with a quiescent state-dominated population when uninjured, followed by a rapid increase in the other cell states in the 0.5-10 days post-injury. At 21 days post-injury, the population is primarily immunomyoblasts and quiescent MuSCs.

Chronic thromboembolic hypertension (CTEPH). CTEPH is a condition that occurs in patients after they have experienced a pulmonary embolism, where the embolism forms scar-like tissue and prevents normal blood flow [71]. Viswanathan *et al.* [71] analyzed tissue from endarterectomy surgeries to find differences between the CTEPH thrombus and healthy cells from nearby tissue. Using trajectory inference, the group was able to show the transition of cell types across pseudotime by examining expression of known cell type markers (e.g., contractile proteins) that then transition to proliferative muscle cells.

Leukemia. Patients with leukemia can develop resistance to chemotherapy or have their cancers return some time after treatment [72]. Li *et al.* [72] identified cell trajectories starting from proliferating stem cells to various cell fates. Leukemia can be further subdivided into FAB subtypes, M0-M7, that indicate the maturity of the cell that the leukemia originates from, with M0 being associated with undifferentiated cells. The earlier subtypes are generally associated with poorer prognoses. In this study, the authors found different proportions of cell states across FAB subtypes. The first group, M0, had a significantly larger proportion of stem cells that had converted into a quiescent state, which the group linked to greater chemoresistance and poor prognosis. The group confirmed their findings with longitudinal samples from five patients, showing that the fraction of quiescent cells doubled in the patient who developed chemoresistance. The authors of this review note that this application of trajectory inference is exemplary; analyzing the data, extracting a hypothesis, then testing it in follow-up experiments is the ideal use of trajectory inference.

Examples of Misuse of Trajectory Inference and Pseudotime

Trajectory inference and pseudotime have names that can easily lead to overinterpretation, implying that the computed trajectories inherently reflect the progression of cells instead of linking cells that have similar gene expression profiles. Similarly, “pseudotime” lends itself to being interpreted as a direct measure of time, even though external information is required to verify that the two are linked. While assembling this review, we encountered a few instances of misrepresentations but most were not sufficiently significant to warrant explicit mention. Below, we discuss some problematic uses of trajectory inference and note pitfalls that should be avoided in future work.

Cao *et al.* [73] investigated the transcriptomic profiles of vascular smooth muscle cells (VSMCs) in the context of aortic aneurysms (AA). The exact cause and mechanisms for them is not known, but involves the weakening and increased porosity of the blood vessel walls, leading to the infiltration of proteins and cells that do not contribute to their mechanical strength [74], [75]. Previous work in VSMCs demonstrated that phenotypic switching [76] was involved with inflammation in chronic kidney disease, suggesting that a similar mechanism could be responsible in AA. As stated by the authors, there is no accepted definition of the different phenotypes with which VSMCs can present; the group specified gene markers for phenotypes of interest and divided the cells accordingly. These VSMC phenotypes consisted of: mesenchymal, T-cell, macrophage, adipocyte, fibroblast, and contractile-like. Between the control and AA conditions, there was a decrease in the proportion of VSMCs and fibroblasts and an increase in the proportion of immune cells.

Trajectory inference. Quoting the paper, *“To identify the origin, trajectory, and timing of differentiation in the VSMC phenotypes, we performed trajectory analysis. From the pseudotime plot and the phenotype-based trajectory plot, we learned that all VSMCs phenotypes were initially derived from contractile VSMCs and fibroblast-like VSMCs [...]”* We note a few things: (1) trajectory inference cannot determine direction, and (2) although a trajectory could connect a particular group with its origin, additional information would be needed to verify it, and (3) pseudotime does not translate to time, so obtaining timing for differentiation is not directly possible. Given that the group used Monocle 2 to perform their trajectory inference, their finding that the different phenotypes derive from contractile VSMCs is most likely due to selecting one as a root cell. The paper goes on to explain the pseudotime position of different phenotypes, suggesting that fibroblast-like VSMCs could be a response to a vascular injury because they happen early in pseudotime, then suggesting suggest that T-cell- and macrophage-like VSMCs could be related to the progression of AA because they happen late in pseudotime. However, selecting a different root cell would result in a different distribution with no changes to the underlying biology; pseudotime does not relate to time. As such, the conclusions drawn from their results are not consistent with what trajectory inference and pseudotime can produce. Extrapolating from their results, the group states, *“Moreover, adipocytes overlapped with mesenchymal VSMCs more than other phenotypes in the cell trajectory plot. Therefore, we believe that these cells are mesenchymal VSMCs that express adipose markers.”* Although the mesenchymal- and adipose-like VSMCs did overlap in pseudotime, examining their positions in

the inferred trajectory shows that they are on different branches; a parallel comparison can be drawn from hematopoiesis: thrombocytes and plasma cells both occur in late pseudotime, but claims about sharing markers would require some elaboration. Lastly, it is not entirely clear whether the subtypes of VSMCs should be connected directly via trajectory inference, as there are notable gaps between the clusters. As previously discussed in the current review, trajectory inference assumes that there is a continuity between cell states in order to produce trajectories; rare states or rapid transitions can make it difficult to detect, but without continuity it is difficult to support that the cells exhibit phenotypic switching.

Liao *et al.* [77] obtained samples from three patients whose kidneys were being removed and performed single-cell RNA sequencing. The data was initially clustered to show all cell states, with proximal tubule (PT) cells further analyzed. The group used Monocle 2 [8] to obtain trajectories for the cells and compute pseudotime, finding a trajectory with two branches. Examining their obtained trajectories, it appears that there is a significant batch effect (Figure 3E), where the different parts of the trajectory are dominated by cells from one donor. Since the figure is showing more than 22,000 points, it is difficult to determine the distribution of donors across the branches, and the distribution is not otherwise discussed. If this is the case, then it indicates that the progression of cell state is related to the particular samples instead of an underlying biological process. When computing pseudotime, there is no mention of how the root is selected, and the published code does not set it explicitly. As such, any state progression could be inverted by selecting a different origin. The figure includes plots for genes across pseudotime but includes all branches along the same pseudotime axis. Although samples on different branches can have the same pseudotime values, they are not immediately comparable since they are supposed to represent different cell states. Consequently, conclusions drawn from the changes in gene expression are not likely to represent changes along either of the two possible trajectories.

Conclusion

Trajectory inference has emerged as a powerful computational approach for unraveling the continuous and dynamic processes underlying cellular differentiation, development, and disease. By introducing different methods such as Monocle, Slingshot, PAGA, and Palantir, our review highlights how these tools not only enable the reconstruction of cellular trajectories from single-cell omics data but also pave the way for a multitude of downstream analyses—from gene regulatory network inference to cross-condition and cross-species comparisons. Yet, as the application examples and misuse cases illustrate, careful consideration of sampling adequacy, continuity assumptions, and the inherent limitations of pseudotime metrics is essential for avoiding overinterpretation. Moving forward, integrating robust external validation, multi-omic data types, and improved methodological frameworks will be crucial for refining these approaches. Ultimately, the continued evolution of trajectory inference will deepen our understanding of cellular behavior in both physiological and pathological contexts, offering promising insights into complex biological processes and disease mechanisms.

Acknowledgements

We thank Felice Information Design for graphic design. This work was funded in part by the NIGMS (R35GM142502).

REFERENCES

- [1] D. Klimmeck *et al.*, “Transcriptome-wide Profiling and Posttranscriptional Analysis of Hematopoietic Stem/Progenitor Cell Differentiation toward Myeloid Commitment,” *Stem Cell Rep.*, vol. 3, no. 5, pp. 858–875, Nov. 2014, doi: 10.1016/j.stemcr.2014.08.012.
- [2] Y. H. Choi and J. K. Kim, “Dissecting Cellular Heterogeneity Using Single-Cell RNA Sequencing,” *Mol. Cells*, vol. 42, no. 3, pp. 189–199, Mar. 2019, doi: 10.14348/molcells.2019.2446.
- [3] J. Ding, N. Sharon, and Z. Bar-Joseph, “Temporal modelling using single-cell transcriptomics,” *Nat. Rev. Genet.*, vol. 23, no. 6, pp. 355–368, Jun. 2022, doi: 10.1038/s41576-021-00444-7.
- [4] W. Saelens, R. Cannoodt, H. Todorov, and Y. Saeys, “A comparison of single-cell trajectory inference methods,” *Nat. Biotechnol.*, vol. 37, no. 5, pp. 547–554, May 2019, doi: 10.1038/s41587-019-0071-9.
- [5] R. C. Gentleman *et al.*, “Bioconductor: open software development for computational biology and bioinformatics,” *Genome Biol.*, vol. 5, no. 10, p. R80, Sep. 2004, doi: 10.1186/gb-2004-5-10-r80.
- [6] K. Street *et al.*, “Slingshot: cell lineage and pseudotime inference for single-cell transcriptomics,” *BMC Genomics*, vol. 19, no. 1, p. 477, Dec. 2018, doi: 10.1186/s12864-018-4772-0.
- [7] C. Trapnell *et al.*, “The dynamics and regulators of cell fate decisions are revealed by pseudotemporal ordering of single cells,” *Nat. Biotechnol.*, vol. 32, no. 4, pp. 381–386, Apr. 2014, doi: 10.1038/nbt.2859.
- [8] X. Qiu *et al.*, “Reversed graph embedding resolves complex single-cell trajectories,” *Nat. Methods*, vol. 14, no. 10, pp. 979–982, Oct. 2017, doi: 10.1038/nmeth.4402.
- [9] K. Campbell, C. P. Ponting, and C. Webber, “Laplacian eigenmaps and principal curves for high resolution pseudotemporal ordering of single-cell RNA-seq profiles,” Sep. 18, 2015, *Bioinformatics*. doi: 10.1101/027219.
- [10] F. A. Wolf *et al.*, “PAGA: graph abstraction reconciles clustering with trajectory inference through a topology preserving map of single cells,” *Genome Biol.*, vol. 20, no. 1, p. 59, Dec. 2019, doi: 10.1186/s13059-019-1663-x.
- [11] J. Cao *et al.*, “The single-cell transcriptional landscape of mammalian organogenesis,” *Nature*, vol. 566, no. 7745, pp. 496–502, Feb. 2019, doi: 10.1038/s41586-019-0969-x.
- [12] L. McInnes, J. Healy, and J. Melville, “UMAP: Uniform Manifold Approximation and Projection for Dimension Reduction,” 2018, *arXiv*. doi: 10.48550/ARXIV.1802.03426.
- [13] Q. Mao, L. Yang, L. Wang, S. Goodison, and Y. Sun, “SimplePPT: A Simple Principal Tree Algorithm,” in *Proceedings of the 2015 SIAM International Conference on Data Mining*, Society for Industrial and Applied Mathematics, Jun. 2015, pp. 792–800. doi: 10.1137/1.9781611974010.89.
- [14] Q. Mao, L. Wang, I. W. Tsang, and Y. Sun, “Principal Graph and Structure Learning Based on Reversed Graph Embedding,” *IEEE Trans. Pattern Anal. Mach. Intell.*, vol. 39, no. 11, pp. 2227–2241, Nov. 2017, doi: 10.1109/TPAMI.2016.2635657.
- [15] M. Setty, V. Kiseliovas, J. Levine, A. Gayoso, L. Mazutis, and D. Pe’er, “Characterization of cell fate probabilities in single-cell data with Palantir,” *Nat. Biotechnol.*, vol. 37, no. 4, pp. 451–460, Apr. 2019, doi: 10.1038/s41587-019-0068-4.
- [16] R. R. Coifman *et al.*, “Geometric diffusions as a tool for harmonic analysis and structure

- definition of data: Diffusion maps,” *Proc. Natl. Acad. Sci.*, vol. 102, no. 21, pp. 7426–7431, May 2005, doi: 10.1073/pnas.0500334102.
- [17] F. Paul *et al.*, “Transcriptional Heterogeneity and Lineage Commitment in Myeloid Progenitors,” *Cell*, vol. 163, no. 7, pp. 1663–1677, Dec. 2015, doi: 10.1016/j.cell.2015.11.013.
- [18] F. A. Wolf, P. Angerer, and F. J. Theis, “SCANPY: large-scale single-cell gene expression data analysis,” *Genome Biol.*, vol. 19, no. 1, p. 15, Dec. 2018, doi: 10.1186/s13059-017-1382-0.
- [19] L. Haghverdi, M. Büttner, F. A. Wolf, F. Buettner, and F. J. Theis, “Diffusion pseudotime robustly reconstructs lineage branching,” *Nat. Methods*, vol. 13, no. 10, pp. 845–848, Oct. 2016, doi: 10.1038/nmeth.3971.
- [20] A. Davis, R. Gao, and N. E. Navin, “SCOPIT: sample size calculations for single-cell sequencing experiments,” *BMC Bioinformatics*, vol. 20, no. 1, p. 566, Dec. 2019, doi: 10.1186/s12859-019-3167-9.
- [21] H. Jeon *et al.*, “Statistical Power Analysis for Designing Bulk, Single-Cell, and Spatial Transcriptomics Experiments: Review, Tutorial, and Perspectives,” *Biomolecules*, vol. 13, no. 2, p. 221, Jan. 2023, doi: 10.3390/biom13020221.
- [22] J. Cao *et al.*, “The single-cell transcriptional landscape of mammalian organogenesis,” *Nature*, vol. 566, no. 7745, pp. 496–502, Feb. 2019, doi: 10.1038/s41586-019-0969-x.
- [23] Q. Meng *et al.*, “Single-Cell Transcriptome Sequencing and Proteomics Reveal Neonatal Ileum Dynamic Developmental Potentials,” *mSystems*, vol. 6, no. 5, p. 10.1128/msystems.00725-21, Oct. 2021, doi: 10.1128/msystems.00725-21.
- [24] A. Pratapa, A. P. Jalihal, J. N. Law, A. Bharadwaj, and T. M. Murali, “Benchmarking algorithms for gene regulatory network inference from single-cell transcriptomic data,” *Nat. Methods*, vol. 17, no. 2, pp. 147–154, Feb. 2020, doi: 10.1038/s41592-019-0690-6.
- [25] D. Song and J. J. Li, “PseudotimeDE: inference of differential gene expression along cell pseudotime with well-calibrated p-values from single-cell RNA sequencing data,” *Genome Biol.*, vol. 22, no. 1, p. 124, Apr. 2021, doi: 10.1186/s13059-021-02341-y.
- [26] A. Deshpande, L.-F. Chu, R. Stewart, and A. Gitter, “Network inference with Granger causality ensembles on single-cell transcriptomics,” *Cell Rep.*, vol. 38, no. 6, p. 110333, Feb. 2022, doi: 10.1016/j.celrep.2022.110333.
- [27] J. Kim, S. T. Jakobsen, K. N. Natarajan, and K.-J. Won, “TENET: gene network reconstruction using transfer entropy reveals key regulatory factors from single cell transcriptomic data,” *Nucleic Acids Res.*, vol. 49, no. 1, pp. e1–e1, Jan. 2021, doi: 10.1093/nar/gkaa1014.
- [28] R. Sung, H. Kim, J. Kim, and D. Lee, “FastTENET: an accelerated TENET algorithm based on manycore computing in Python,” *Bioinformatics*, vol. 40, no. 12, p. btae699, Nov. 2024, doi: 10.1093/bioinformatics/btae699.
- [29] W. Hou, Z. Ji, Z. Chen, E. J. Wherry, S. C. Hicks, and H. Ji, “A statistical framework for differential pseudotime analysis with multiple single-cell RNA-seq samples,” *Nat. Commun.*, vol. 14, no. 1, p. 7286, Nov. 2023, doi: 10.1038/s41467-023-42841-y.
- [30] R. Sugihara, Y. Kato, T. Mori, and Y. Kawahara, “Alignment of single-cell trajectory trees with CAPITAL,” *Nat. Commun.*, vol. 13, no. 1, p. 5972, Oct. 2022, doi: 10.1038/s41467-022-33681-3.
- [31] E. A. Woodcock and S. J. Matkovich, “Cardiomyocytes structure, function and associated pathologies,” *Int. J. Biochem. Cell Biol.*, vol. 37, no. 9, pp. 1746–1751, Sep. 2005, doi: 10.1016/j.biocel.2005.04.011.
- [32] S. Kannan *et al.*, “Trajectory reconstruction identifies dysregulation of perinatal maturation programs in pluripotent stem cell-derived cardiomyocytes,” *Cell Rep.*, vol. 42, no. 4, p. 112330, Apr. 2023, doi: 10.1016/j.celrep.2023.112330.
- [33] A. L. Koenig *et al.*, “Single-cell transcriptomics reveals cell-type-specific diversification in

- human heart failure,” *Nat. Cardiovasc. Res.*, vol. 1, no. 3, pp. 263–280, Mar. 2022, doi: 10.1038/s44161-022-00028-6.
- [34] L. Ma *et al.*, “Single-Cell RNA Sequencing and Quantitative Proteomics Analysis Elucidate Marker Genes and Molecular Mechanisms in Hypoplastic Left Heart Patients With Heart Failure,” *Front. Cell Dev. Biol.*, vol. 9, p. 617853, Feb. 2021, doi: 10.3389/fcell.2021.617853.
- [35] R. Satija, J. A. Farrell, D. Gennert, A. F. Schier, and A. Regev, “Spatial reconstruction of single-cell gene expression data,” *Nat. Biotechnol.*, vol. 33, no. 5, pp. 495–502, May 2015, doi: 10.1038/nbt.3192.
- [36] A. Butler, P. Hoffman, P. Smibert, E. Papalexi, and R. Satija, “Integrating single-cell transcriptomic data across different conditions, technologies, and species,” *Nat. Biotechnol.*, vol. 36, no. 5, pp. 411–420, May 2018, doi: 10.1038/nbt.4096.
- [37] T. Stuart *et al.*, “Comprehensive Integration of Single-Cell Data,” *Cell*, vol. 177, no. 7, pp. 1888–1902.e21, Jun. 2019, doi: 10.1016/j.cell.2019.05.031.
- [38] Y. Hao *et al.*, “Integrated analysis of multimodal single-cell data,” *Cell*, vol. 184, no. 13, pp. 3573–3587.e29, Jun. 2021, doi: 10.1016/j.cell.2021.04.048.
- [39] Y. Hao *et al.*, “Dictionary learning for integrative, multimodal and scalable single-cell analysis,” *Nat. Biotechnol.*, vol. 42, no. 2, pp. 293–304, Feb. 2024, doi: 10.1038/s41587-023-01767-y.
- [40] M. Ashburner *et al.*, “Gene Ontology: tool for the unification of biology,” *Nat. Genet.*, vol. 25, no. 1, pp. 25–29, May 2000, doi: 10.1038/75556.
- [41] The Gene Ontology Consortium *et al.*, “The Gene Ontology knowledgebase in 2023,” *GENETICS*, vol. 224, no. 1, p. iyad031, May 2023, doi: 10.1093/genetics/iyad031.
- [42] M. Kanehisa, “KEGG: Kyoto Encyclopedia of Genes and Genomes,” *Nucleic Acids Res.*, vol. 28, no. 1, pp. 27–30, Jan. 2000, doi: 10.1093/nar/28.1.27.
- [43] M. Kanehisa, “Toward understanding the origin and evolution of cellular organisms,” *Protein Sci.*, vol. 28, no. 11, pp. 1947–1951, Nov. 2019, doi: 10.1002/pro.3715.
- [44] M. Kanehisa, M. Furumichi, Y. Sato, Y. Matsuura, and M. Ishiguro-Watanabe, “KEGG: biological systems database as a model of the real world,” *Nucleic Acids Res.*, vol. 53, no. D1, pp. D672–D677, Jan. 2025, doi: 10.1093/nar/gkae909.
- [45] Y. Yoshimura *et al.*, “A single-cell multiomic analysis of kidney organoid differentiation,” *Proc. Natl. Acad. Sci.*, vol. 120, no. 20, p. e2219699120, May 2023, doi: 10.1073/pnas.2219699120.
- [46] F. D. Debelle, J.-L. Vanherweghem, and J. L. Nortier, “Aristolochic acid nephropathy: A worldwide problem,” *Kidney Int.*, vol. 74, no. 2, pp. 158–169, Jul. 2008, doi: 10.1038/ki.2008.129.
- [47] J. Chen *et al.*, “Integrated single-cell transcriptomics and proteomics reveal cellular-specific responses and microenvironment remodeling in aristolochic acid nephropathy,” *JCI Insight*, vol. 7, no. 16, p. e157360, Aug. 2022, doi: 10.1172/jci.insight.157360.
- [48] Y. Kirita, H. Wu, K. Uchimura, P. C. Wilson, and B. D. Humphreys, “Cell profiling of mouse acute kidney injury reveals conserved cellular responses to injury,” *Proc. Natl. Acad. Sci.*, vol. 117, no. 27, pp. 15874–15883, Jul. 2020, doi: 10.1073/pnas.2005477117.
- [49] J. W. Hickey *et al.*, “Organization of the human intestine at single-cell resolution,” *Nature*, vol. 619, no. 7970, pp. 572–584, Jul. 2023, doi: 10.1038/s41586-023-05915-x.
- [50] T. Wälchli *et al.*, “Single-cell atlas of the human brain vasculature across development, adulthood and disease,” *Nature*, vol. 632, no. 8025, pp. 603–613, Aug. 2024, doi: 10.1038/s41586-024-07493-y.
- [51] A. Pichet Binette *et al.*, “Proteomic changes in Alzheimer’s disease associated with progressive A β plaque and tau tangle pathologies,” *Nat. Neurosci.*, vol. 27, no. 10, pp. 1880–1891, Oct. 2024, doi: 10.1038/s41593-024-01737-w.
- [52] R. Cannoodt *et al.*, “SCORPIUS improves trajectory inference and identifies novel modules in dendritic cell development,” Oct. 06, 2016, *Bioinformatics*. doi: 10.1101/079509.

- [53] S. Mukherjee *et al.*, “Molecular estimation of neurodegeneration pseudotime in older brains,” *Nat. Commun.*, vol. 11, no. 1, p. 5781, Nov. 2020, doi: 10.1038/s41467-020-19622-y.
- [54] D. L. Dai, M. Li, and E. B. Lee, “Human Alzheimer’s disease reactive astrocytes exhibit a loss of homeostatic gene expression,” *Acta Neuropathol. Commun.*, vol. 11, no. 1, p. 127, Aug. 2023, doi: 10.1186/s40478-023-01624-8.
- [55] S. Smajić *et al.*, “Single-cell sequencing of human midbrain reveals glial activation and a Parkinson-specific neuronal state,” *Brain*, vol. 145, no. 3, pp. 964–978, Apr. 2022, doi: 10.1093/brain/awab446.
- [56] J. Lotto *et al.*, “Single-Cell Transcriptomics Reveals Early Emergence of Liver Parenchymal and Non-parenchymal Cell Lineages,” *Cell*, vol. 183, no. 3, pp. 702-716.e14, Oct. 2020, doi: 10.1016/j.cell.2020.09.012.
- [57] L. Tosti *et al.*, “Single-Nucleus and In Situ RNA–Sequencing Reveal Cell Topographies in the Human Pancreas,” *Gastroenterology*, vol. 160, no. 4, pp. 1330-1344.e11, Mar. 2021, doi: 10.1053/j.gastro.2020.11.010.
- [58] Y. Xin *et al.*, “Pseudotime Ordering of Single Human β -Cells Reveals States of Insulin Production and Unfolded Protein Response,” *Diabetes*, vol. 67, no. 9, pp. 1783–1794, Sep. 2018, doi: 10.2337/db18-0365.
- [59] D. Cui Zhou *et al.*, “Spatially restricted drivers and transitional cell populations cooperate with the microenvironment in untreated and chemo-resistant pancreatic cancer,” *Nat. Genet.*, vol. 54, no. 9, pp. 1390–1405, Sep. 2022, doi: 10.1038/s41588-022-01157-1.
- [60] K. Bao *et al.*, “Pseudotime Ordering Single-Cell Transcriptomic of β Cells Pancreatic Islets in Health and Type 2 Diabetes,” *Phenomics*, vol. 1, no. 5, pp. 199–210, Oct. 2021, doi: 10.1007/s43657-021-00024-z.
- [61] D. D. Scripture-Adams *et al.*, “Single nuclei transcriptomics of muscle reveals intra-muscular cell dynamics linked to dystrophin loss and rescue,” *Commun. Biol.*, vol. 5, no. 1, p. 989, Sep. 2022, doi: 10.1038/s42003-022-03938-0.
- [62] P. Chen *et al.*, “Diversity and intratumoral heterogeneity in human gallbladder cancer progression revealed by single-cell RNA sequencing,” *Clin. Transl. Med.*, vol. 11, no. 6, p. e462, Jun. 2021, doi: 10.1002/ctm2.462.
- [63] Y. Zhang *et al.*, “Single-cell RNA-seq reveals transcriptional landscape and intratumor heterogeneity in gallbladder cancer liver metastasis microenvironment,” *Ann. Transl. Med.*, vol. 9, no. 10, pp. 889–889, May 2021, doi: 10.21037/atm-21-2227.
- [64] Y. Zhang *et al.*, “Single-cell RNA-sequencing atlas reveals an MDK-dependent immunosuppressive environment in ErbB pathway-mutated gallbladder cancer,” *J. Hepatol.*, vol. 75, no. 5, pp. 1128–1141, Nov. 2021, doi: 10.1016/j.jhep.2021.06.023.
- [65] Y. Zhang *et al.*, “Single-cell characterization of infiltrating T cells identifies novel targets for gallbladder cancer immunotherapy,” *Cancer Lett.*, vol. 586, p. 216675, Apr. 2024, doi: 10.1016/j.canlet.2024.216675.
- [66] C. Li, W. Song, J. Zhang, and Y. Luo, “Single-cell transcriptomics reveals heterogeneity in esophageal squamous epithelial cells and constructs models for predicting patient prognosis and immunotherapy,” *Front. Immunol.*, vol. 14, p. 1322147, Nov. 2023, doi: 10.3389/fimmu.2023.1322147.
- [67] The Cancer Genome Atlas Research Network *et al.*, “The Cancer Genome Atlas Pan-Cancer analysis project,” *Nat. Genet.*, vol. 45, no. 10, pp. 1113–1120, Oct. 2013, doi: 10.1038/ng.2764.
- [68] G. Fitzgerald *et al.*, “MME+ fibro-adipogenic progenitors are the dominant adipogenic population during fatty infiltration in human skeletal muscle,” *Commun. Biol.*, vol. 6, no. 1, p. 111, Jan. 2023, doi: 10.1038/s42003-023-04504-y.
- [69] S. N. Oprescu, F. Yue, J. Qiu, L. F. Brito, and S. Kuang, “Temporal Dynamics and Heterogeneity of Cell Populations during Skeletal Muscle Regeneration,” *iScience*, vol. 23, no. 4, p. 100993, Apr. 2020, doi: 10.1016/j.isci.2020.100993.

- [70]B. Malecova *et al.*, “Dynamics of cellular states of fibro-adipogenic progenitors during myogenesis and muscular dystrophy,” *Nat. Commun.*, vol. 9, no. 1, p. 3670, Sep. 2018, doi: 10.1038/s41467-018-06068-6.
- [71]G. Viswanathan *et al.*, “Single-Cell Analysis Reveals Distinct Immune and Smooth Muscle Cell Populations that Contribute to Chronic Thromboembolic Pulmonary Hypertension,” *Am. J. Respir. Crit. Care Med.*, vol. 207, no. 10, pp. 1358–1375, May 2023, doi: 10.1164/rccm.202203-0441OC.
- [72]K. Li *et al.*, “Single-cell analysis reveals the chemotherapy-induced cellular reprogramming and novel therapeutic targets in relapsed/refractory acute myeloid leukemia,” *Leukemia*, vol. 37, no. 2, pp. 308–325, Feb. 2023, doi: 10.1038/s41375-022-01789-6.
- [73]G. Cao *et al.*, “Single-cell RNA sequencing reveals the vascular smooth muscle cell phenotypic landscape in aortic aneurysm,” *Cell Commun. Signal.*, vol. 21, no. 1, p. 113, May 2023, doi: 10.1186/s12964-023-01120-5.
- [74]E. Branchetti *et al.*, “Oxidative stress modulates vascular smooth muscle cell phenotype via CTGF in thoracic aortic aneurysm,” *Cardiovasc. Res.*, vol. 100, no. 2, pp. 316–324, Nov. 2013, doi: 10.1093/cvr/cvt205.
- [75]C. Behr Andersen *et al.*, “Abdominal Aortic Aneurysms Growth Is Associated With High Concentrations of Plasma Proteins in the Intraluminal Thrombus and Diseased Arterial Tissue,” *Arterioscler. Thromb. Vasc. Biol.*, vol. 38, no. 9, pp. 2254–2267, Sep. 2018, doi: 10.1161/ATVBAHA.117.310126.
- [76]A. L. Durham, M. Y. Speer, M. Scatena, C. M. Giachelli, and C. M. Shanahan, “Role of smooth muscle cells in vascular calcification: implications in atherosclerosis and arterial stiffness,” *Cardiovasc. Res.*, vol. 114, no. 4, pp. 590–600, Mar. 2018, doi: 10.1093/cvr/cvy010.
- [77]J. Liao *et al.*, “Single-cell RNA sequencing of human kidney,” *Sci. Data*, vol. 7, no. 1, p. 4, Jan. 2020, doi: 10.1038/s41597-019-0351-8.